Automated Design Exploration of the TALOS WEC Using the Novel TOP-WEC Software Stack

David Ogden, Salman Husain, Aidan Bharath, Jochem Weber, Wanan Sheng and George Aggidis

***Abstract*—Despite numerous prototype deployments, many wave energy converter (WEC) developers have struggled to achieve sufficient power production for commercial viability—in part due to the lack of rigorous early-stage design exploration and optimization—leading to premature convergence on suboptimal designs. To address this challenge, we present an automated design exploration study of TALOS, a promising multi-axis WEC concept developed by Lancaster University. Using the TOP-WEC framework (Toolkit for Optimizing the Performance of WECs)—which integrates automated meshing, Capytaine for hydrodynamics, and HydroChrono time-domain simulation built on Project Chrono—we systematically evaluate a range of geometric and power take-off configurations. The TOP-WEC framework's foundation on generalized numerical modeling tools enables its application across a broad range of WEC concepts, providing a versatile platform for automated design studies. Leveraging automated simulations and structured design exploration routines, we assess multiple design variants against a baseline TALOS WEC to quantify performance improvements, such as a 20% increase in capture width ratio and 15% improvement in power/volume for specific configurations. This work underscores the importance of comprehensive numerical modeling and automation in advancing WEC technologies toward viable commercial deployment. This paper presents a pre-optimization exploration, laying the foundation for future optimization studies and high-fidelity validation under the *SEA-Stack* project.**

***Index Terms*—Wave Energy Converter, Hydrodynamic Modeling, Automated Design Exploration, TOP-WEC, SEA-Stack**

I. Introduction

Wave energy represents a significant global energy resource [1], yet deployment still lags well behind wind and solar [2]. High levelized cost of energy (LCOE) and substantial reliability risks in harsh marine environments remain the principal barriers [3]. LCOE is driven by the ratio between lifetime energy production and the capital invested in the device structure and power-take-off (PTO) system [1]; maximizing energy capture is therefore paramount. Progress has been hindered, in part by insufficient design exploration at low technology readiness levels. Without rigorous numerical evaluation, developers risk converging on sub-optimal configurations [3], advancing concepts with limited intrinsic performance into expensive prototypes that underperform and erode investor confidence [4]. Effective WEC development therefore hinges on *co-design*—the simultaneous optimization of geometry, mechanical topology, PTO parameters, and control strategy.

A. The Role of Design Exploration in WEC Development

Before applying optimization techniques, it is critical to conduct structured design exploration to better understand device behavior and establish meaningful bounds on the design space. Key benefits include:

- Identifying high-leverage parameters through sensitivity analysis.
- Developing engineering intuition around system behavior and performance trade-offs.
- Defining appropriate performance metrics for future optimization.
- Avoiding premature convergence on suboptimal configurations.
- Informing the setup of formal optimization algorithms with realistic bounds and constraints.
- Building confidence in numerical models through systematic validation.
- Establishing which aspects of the system warrant optimization focus.

Because hydrodynamics, PTO mechanics, and control interact nonlinearly—particularly for resonant archetypes [5], [6]—sequential optimization is inevitably suboptimal [7]. Comprehensive numerical design-space exploration at early technology readiness levels remains the only cost-effective route to identify concepts with high techno-economic potential [6], [8], [9]. Early work by McCabe [10] and McCabe et al. [11] demonstrated this potential through automated optimization of surge–pitch collectors using genetic algorithms, achieving 30–45% improvements in power absorption relative to manually tuned baselines. These results reinforce the central claim of this paper: fully

This work was supported by the U.S. Department of Energy (DOE) Water Power Technologies Office (WPTO) through the Testing Expertise and Access for Marine Energy Research (TEAMER) program, administered by the Pacific Ocean Energy Trust (POET). This work was authored in part by the National Renewable Energy Laboratory for the U.S. Department of Energy (DOE) under Contract No. DE-AC36-08GO28308. Funding provided by U.S. Department of Energy Office of Energy Efficiency and Renewable Energy Water Power Technologies Office. The views expressed in the article do not necessarily represent the views of the DOE or the U.S. Government. The U.S. Government retains and the publisher, by accepting the article for publication, acknowledges that the U.S. Government retains a nonexclusive, paid-up, irrevocable, worldwide license to publish or reproduce the published form of this work, or allow others to do so, for U.S. Government purposes.

David Ogden is with Simocean and was formerly with the National Renewable Energy Laboratory (NREL). Email: david [at] simocean [dot] xyz

Salman Husain, Aidan Bharath, and Jochem Weber are with NREL.

Wanan Sheng is with South East Technological University, Ireland.

George Aggidis is with Lancaster University.

Digital Object Identifier: https://doi.org/10.36688/1113

integrated, open-source toolchains are essential if WEC designers are to explore the vast coupled design space efficiently and bring LCOE below commercial thresholds.

This vision has been evolving for decades, beginning with David Pizer's 1994 work on numerical modeling of wave energy absorbers [12]. Through systematic numerical exploration—performing over 150 power absorption calculations across various geometries and control strategies—Pizer demonstrated that computational methods could achieve a level of comprehensive study that would be impractical through physical testing alone.

Stephen Salter articulated the community's ambition in his 2016 review of wave energy development, where he reflected on the evolution of design tools from physical testing to numerical simulation:

> "It has been a long-term dream to design and test wave-power devices in a computer with seamless links between the original drawing and the final results and with new ideas tried as quickly as Jamie Taylor could change models in a narrow tank. It is still a dream, but we may be getting closer." [13]

The TOP-WEC framework represents a significant step toward realizing this vision of enabling automated design exploration that approaches the speed and flexibility of physical model testing. As we move closer to this vision, the challenge shifts from building the simulation tools themselves toward using them effectively to balance computational power with interpretability and ensure that automated design exploration builds rather than erodes developer confidence.

B. Workflow Fragmentation: The Integration Bottleneck

In current practice, geometry is typically meshed manually with proprietary CAD software such as SolidWorks or Cubit. Hydrodynamic coefficients are generated by frequency-domain boundary element method (BEM) solvers written in FORTRAN but accessed through Python wrappers (*WAMIT*, *NEMOH*, *Capytaine*) [14], and time-domain dynamics are simulated in the MATLAB/Simulink-based *WEC-Sim* [15]. Data must pass through *BEMIO* to become an HDF5 file compatible with *WEC-Sim* [16], [17]. This Python $\leftrightarrow$ FORTRAN $\leftrightarrow$ MATLAB approach introduces license costs, incompatible formats, manual scripts, and significant *integration friction* [18]. Every geometry change triggers re-meshing, fresh BEM analysis, data conversion, and a new time-domain run, increasing setup and computation time [19], [20].

A 2022 review of WEC-Sim usage patterns revealed that users rarely explore the geometry design space [18], despite overwhelming research evidence that geometric optimization is crucial for WEC performance. Even when geometry exploration is attempted, the process is cumbersome due to the need to manually handle geometry changes, re-meshing, and data conversion between tools [21]. This gap between research insights and practical application highlights the need for tools that make design exploration more accessible and intuitive. While *WEC-Sim* excels for control studies and offers PTO-Sim and Simscape Multibody capabilities [22]–[24], its limited interoperability with meshing and BEM tools and proprietary licenses hinders its effectiveness for large-scale co-design studies. Furthermore, the lack of a unified workflow for design makes it very challenging to validate designs generated by the optimization process, as there is no clear route from reduced-order modeling to the high-fidelity modeling required to build confidence in the results.

C. The TOP-WEC Framework and SEA-Stack Integration

To eliminate these bottlenecks, we present **TOP-WEC** (Toolkit for Optimizing the Performance of Wave Energy Converters): a stack of open-source codes that provide a unified workflow for WEC design space exploration. While TOP-WEC still uses .h5 files for hydrodynamic data (the same format as WEC-Sim), the key improvement is that the entire workflow is orchestrated through Python scripts. This enables seamless automation from geometry definition through to time-domain simulation results, eliminating the manual intervention and integration friction that currently hinders rapid design iteration.

The framework is designed as the first tier in a multi-fidelity modeling pathway within the broader SEA-Stack initiative. This staged approach enables rapid concept development while maintaining a clear path to high-fidelity validation. Once promising designs are identified through parameter studies or optimization, they can be seamlessly transferred to higher-fidelity solvers—such as OpenFOAM or DualSPHysics—for validation of complex nonlinear behavior.

TABLE I
COMPARISON OF *WEC-Sim* AND *TOP-WEC* FOR AUTOMATED DESIGN EXPLORATION.

Aspect	WEC-Sim	TOP-WEC
Environment	MATLAB / Simulink	Python / C++
Hydro Input	External BEM via BEMIO	Direct API (Capytaine)
Workflow	Manual, fragmented	Unified, automated
Automation	Limited	High
Licensing	Proprietary	Open-source
Cost	High (license)	Free
Speed	Moderate	High
Maturity	Mature, widely used	Experimental, under development

In summary, TOP-WEC represents a significant step toward realizing Salter's vision of seamless design exploration—where new ideas can be tested as quickly as changing models in a wave tank. While the framework enables high-throughput, early-stage co-design of geometry and PTO parameters, this paper focuses on demonstrating its capabilities through systematic single-variable studies of the TALOS multi-axis point absorber. These studies provide valuable insights into parameter sensitivities and trade-offs, laying the groundwork for future multi-parameter optimization studies.

D. The TALOS WEC as a Test Case

The TALOS WEC serves as an ideal test case for demonstrating TOP-WEC's capabilities. Its multi-axis architecture and complex geometry provide a challenging yet representative example for evaluating the framework's performance. The device's design features, including its tapered profile and multiple PTO units, allow us to explore a wide range of geometric and control parameters, making it well-suited for demonstrating the value of systematic design exploration.

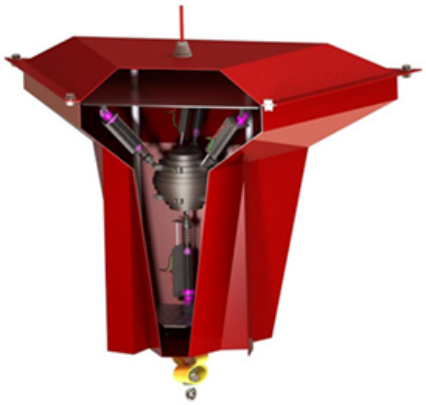

Fig. 1. Cutaway rendering of the TALOS WEC concept, showing the multi-axis PTO arrangement and internal reaction mass. Image credit: Lancaster University [25].

II. The TOP-WEC Framework

A. Overview and Design Methodology

The TOP-WEC framework integrates multiple open-source tools into a unified workflow for geometry generation, hydrodynamic modeling, and time-domain simulation. The core components include:

- Bespoke Python scripts for structured mesh generation
- Capytaine, a Python-native BEM solver [26]
- HydroChrono, a time-domain dynamics engine built on Project Chrono [27]

Each step—mesh generation, BEM analysis with Capytaine, data conversion, and HydroChrono simulation—is controlled programmatically, ensuring consistent inputs and enabling parallel processing. This represents a significant advancement over existing manual workflows, where each step requires separate intervention and careful data management.

By systematically building confidence in the numerical models through preliminary design exploration, we can make more informed decisions about which aspects of the system warrant optimization focus and which parameters have the most significant impact on performance.

Eventually, the SEA-Stack project will support seamless transitions to high-fidelity modeling. This capability allows for rapid design iteration *and* validation, ensuring that optimization results are both physically realistic and practically implementable. Additionally, being able to seamlessly transition a WEC model from potential flow to computational fluid dynamics in the future will enable us to rapidly obtain drag coefficients, to incorporate viscous effects in our analysis more easily.

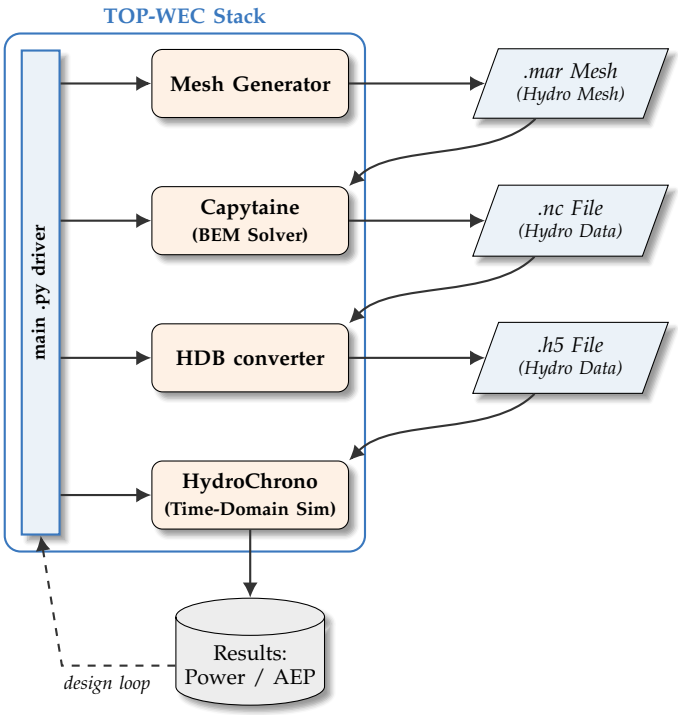

Fig. 2. TOP-WEC simulation stack. The workflow is orchestrated by a Python script, which sequentially executes mesh generation, hydrodynamic modeling, and time-domain simulation. Intermediate outputs are stored and reused to support design iteration.

B. Simulation Approach

The use of HydroChrono is critical for capturing fully nonlinear multibody dynamics in the time domain. This allows for the computation of power output time series for each PTO unit, providing detailed insights into the device's performance. For this study, we focus on regular wave simulations, which are particularly useful during early-stage WEC development. Regular waves allow for broad design exploration across a wide range of parameters, producing results that are intuitive and easy to interpret. This approach helps in quickly understanding how the design behaves and responds to specific design changes, providing valuable insights before moving on to more complex sea states.

By simulating the TALOS WEC in HydroChrono, we can analyze the dynamic interactions between the hull and the internal reaction mass, as well as the performance of each PTO unit. This capability is particularly valuable for the TALOS design, which features multiple PTO units that can be independently optimized.

C. Geometry Meshing

Custom Python scripts are used to procedurally generate structured surface meshes for the WEC geometry. These routines allow parametric control over geometry

and panel density and are designed to balance numerical accuracy with computational cost. Key design parameters include:

- Number of sides and radii of top and bottom polygonal cross sections
- Straight draft depth and taper draft height
- Nose curvature via vertex deformations (controlled by a control point on the leading edge)
- Panel clustering via cosine spacing.

The mesh generator constructs a layered body by interpolating between top, middle, and bottom cross sections. Polygonal edges are subdivided using either linear or cosine spacing. Cosine spacing clusters panels near boundaries or corners, where hydrodynamic quantities vary most rapidly. This is implemented using the transformation:

$$s_i = \frac{1 - \cos\left(\frac{i\pi}{n}\right)}{2}, \qquad i = 0, \ldots, n \tag{1}$$

where s_i are normalized panel positions from 0 to 1, and n is the number of intervals. This function is used in both the vertical (draft) direction and along curved surfaces. Figure 3 illustrates how this scheme results in finer panel resolution near surface extremes.

a) Polygonal Subdivision and Mesh Generation: Each cross section is defined in the $x - y$ plane at a given z-coordinate and initialized as a regular N-gon (e.g., a hexagon or octagon). The `subdivide_edge()` function interpolates the polygon edges using either uniform or cosine spacing. These subdivided layers are then stacked and connected along the z-axis, forming quadrilateral panels between corresponding points. Distinct meshing logic is applied to handle the tapering region, the straight-draft extension, and the bottom endcap, where additional radial subdivisions are introduced to cover the base surface.

The final mesh is exported in both `.mar` format for Nemoh and `.obj` format for visualization. The mesh is also translated to align with the center of gravity of the hull.

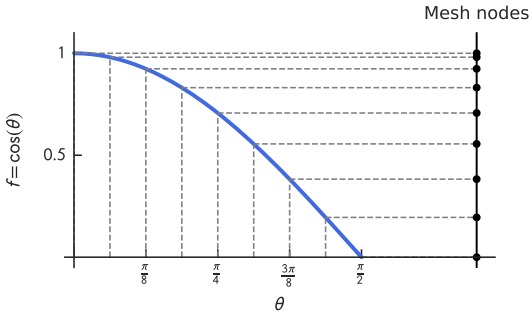

Fig. 3. Illustration of cosine panel spacing. Equally spaced samples along the θ axis are mapped vertically using $f = \cos(\theta)$, producing tighter node clustering near boundaries. This ensures resolution where diffraction and radiation effects are strongest.

D. Hydrodynamic Modeling with Capytaine

Capytaine solves the linearized potential flow problem using BEM in the frequency domain. Assuming an inviscid, incompressible, and irrotational fluid, the complex velocity potential Φ satisfies Laplace's equation:

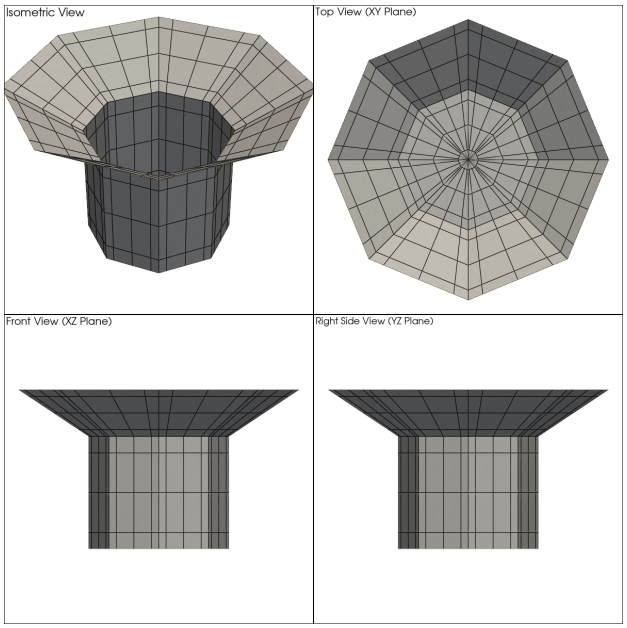

Fig. 4. TALOS mesh generated from the meshing script, showing quadrilateral panels and geometry taper. Views are shown in isometric (top left), top (top right), front (bottom left), and side (bottom right) orientations. These structured panels are used as input to the boundary element solver.

$$\nabla^2 \Phi = 0 \tag{2}$$

For each angular frequency ω, two boundary value problems are solved:

- **Radiation problem:** The body oscillates in one rigid-body mode j with no incident wave. The resulting velocity potential Φ_j^{rad} yields added mass and radiation damping.
- **Diffraction problem:** The body is held fixed while a plane wave of frequency ω and heading β impinges upon it, generating the diffraction potential Φ^{diff}.

From the radiation problem, the added mass, $A_{ij}(\omega)$, and damping, $B_{ij}(\omega)$, coefficients for motions i and j are computed by integrating the hydrodynamic pressure over the wetted surface, S_B, where ρ is the fluid density:

$$A_{ij}(\omega) = -\frac{\rho}{\omega} \int_{S_B} \Im[\Phi_j^{\text{rad}}]\, \mathbf{n} \cdot \delta\mathbf{r}_i \, dS \tag{3}$$

$$B_{ij}(\omega) = \rho \int_{S_B} \Re[\Phi_j^{\text{rad}}]\, \mathbf{n} \cdot \delta\mathbf{r}_i \, dS \tag{4}$$

where $\delta\mathbf{r}_i$ is the velocity field corresponding to unit motion in mode i, and $\mathbf{n}$ is the outward surface normal.

The excitation force in mode i is derived from the diffraction potential:

$$F_i^{\text{exc}}(\omega, \beta) = -\rho i\omega \int_{S_B} \Phi^{\text{diff}}\, \mathbf{n} \cdot \delta\mathbf{r}_i \, dS \tag{5}$$

where $\eta(t)$ is the free-surface elevation. Hydrostatic restoring coefficients K_{ij} are computed from the dis-

placed volume and pressure distribution in the equilibrium position.

Capytaine discretizes these boundary integrals using panel meshes and assembles the hydrodynamic quantities into a frequency-dependent dataset stored in NetCDF format.

E. Time-Domain Simulation with HydroChrono

HydroChrono is a C++-based simulation framework built on the Chrono::Engine physics engine. In this work, it is controlled via Python scripting to simulate the TALOS WEC, which consists of a surface-piercing hull and an internal reaction mass—a dense spherical body—connected by multiple PTO units. HydroChrono integrates rigid-body dynamics, time-domain hydrodynamic forces, and mechanical constraints into a unified time-domain solver.

a) Governing Equations: Hydrodynamic forces are incorporated using the Cummins equation, which captures the memory effect of radiation forces through a convolution integral:

$$\mathbf{M}\ddot{\mathbf{x}}(t) = -\int_0^t \mathbf{K}_{\text{rad}}(t-\tau)\dot{\mathbf{x}}(\tau)\,d\tau + \mathbf{F}_{\text{exc}}(t) + \mathbf{F}_{\text{other}}(t) \quad (6)$$

Here, $\mathbf{M}$ is the total inertia matrix, including added mass at infinite frequency. The term $\mathbf{K}_{\text{rad}}(t)$ is the radiation impulse response function (IRF), and $\mathbf{F}_{\text{exc}}(t)$ is the wave excitation force. Both are derived from the frequency-domain hydrodynamic coefficients computed by Capytaine.

The radiation IRF, $\mathbf{K}_{\text{rad}}(t)$, is obtained from the radiation damping matrix, $\mathbf{B}(\omega)$, using:

$$\mathbf{K}_{\text{rad}}(t) = \frac{2}{\pi}\int_0^\infty \mathbf{B}(\omega)\cos(\omega t)\,d\omega \quad (7)$$

Similarly, the excitation force in the time domain is computed by convolving the wave elevation, $\eta(t)$, with the excitation IRF, $\mathbf{k}_{\text{exc}}(t)$, defined from the frequency-domain excitation force, $\mathbf{F}_{\text{exc}}(\omega)$:

$$\mathbf{F}_{\text{exc}}(t) = \int_0^t \mathbf{k}_{\text{exc}}(t-\tau)\,\eta(\tau)\,d\tau \quad (8)$$

$$\mathbf{k}_{\text{exc}}(t) = \frac{1}{\pi}\int_0^\infty \Re\left[\mathbf{F}_{\text{exc}}(\omega)\right]\cos(\omega t)\,d\omega \quad (9)$$

This approach enables accurate reconstruction of frequency-domain effects in time-domain simulations, allowing HydroChrono to solve the full Cummins equation using Chrono's native multibody solver.

b) Modeling the TALOS Architecture: TALOS is modeled as a coupled two-body system:

- The **hull** is treated as a hydrodynamic body, with precomputed added mass, radiation damping, hydrostatic restoring forces, and wave excitation.
- The **internal sphere** represents a concentrated reaction mass and is modeled as a non-hydrodynamic rigid body. Its mass and inertia are computed from the desired ballast ratio and assumed material density (e.g., lead).

The two bodies are connected via six **multi-axis PTO units**, implemented as linear spring–damper actuators. Each PTO unit is defined by its stiffness, damping, and two attachment points—one on the hull and one on the sphere—allowing for varied geometries and orientations.

Listing 1. Example of a single PTO unit definition.

```
pto(1) = ptoClass('LinSpringDamper');
pto(1).stiffness = 2.5e6;
pto(1).damping = 1.0e6;
pto(1).rest_length = 1.0;
pto(1).bodies = [body(1), body(2)];
pto(1).attachments = [
   [15.0, 0.0, -8.66],
   [2.5, 0.0, -4.33]
];
```

c) Simulation Pipeline: The modeling workflow consists of:

1) Generating panelized meshes and computing hydrodynamic coefficients with Capytaine.
2) Transforming frequency-domain outputs into time-domain impulse response functions and exporting to HDF5.
3) Defining the HydroChrono model via Python, including mass properties, PTO definitions, and wave conditions.
4) Solving the coupled dynamics with Chrono, which integrates all forces using a variational time integrator.

d) Key Features:

- Direct enforcement of the full Cummins equation within Chrono's multibody dynamics solver.
- Modular PTO definitions enable rapid testing of different actuator layouts and control laws.
- Python-driven simulation setup streamlines the design–evaluate loop across a wide range of TALOS configurations.

TOP-WEC is under active development as part of the open-source SEA-Stack ecosystem. In this broader framework, TOP-WEC serves as the fast-iteration, reduced-order modeling tier. The vision is for candidate designs generated from parameter sweeps or optimization to eventually be transferred to higher-fidelity solvers—such as Project Chrono coupled to OpenFOAM or Dual-SPHysics—for validation of potential flow results and estimation of drag coefficients. This staged modeling approach ims to build confidence among developers and reduce the cost of design failure.

III. TALOS Case Study and Results

A. Regular Wave Simulations

The initial design exploration uses regular wave simulations to systematically evaluate the impact of geometric variations on device performance. This method provides clear insights into the relationship between design parameters and power capture efficiency, while also offering rapid turnaround—each design iteration, including re-meshing, hydrodynamic coefficient computation, and time-domain simulation, can be completed in under one minute. This fast feedback enables efficient exploration of the design space, allowing the

team to quickly refine concepts and avoid expending significant time and computational resources on less promising directions. The regular wave analysis in this study focuses on:

- **Straight draft depth:** 8–12 m
- **Taper draft height:** 2.5–10 m
- **Top radius:** 13–19 m
- **Nose shape:** variation in leading x-position

For each design, we evaluate:
The two primary performance metrics are:

- **Capture width ratio (CWR):**

$$\mathrm{CWR} = \frac{P_{\mathrm{abs}}}{J \cdot w} \tag{10}$$

where P_{abs} is the absorbed power (W), J is the incident wave power flux per unit width (W/m), and w is the device width (m).

- **Average power per unit volume:**

$$P_{\mathrm{vol}} = \frac{P_{\mathrm{abs}}}{V} \tag{11}$$

where V is the submerged volume of the device (m^3).

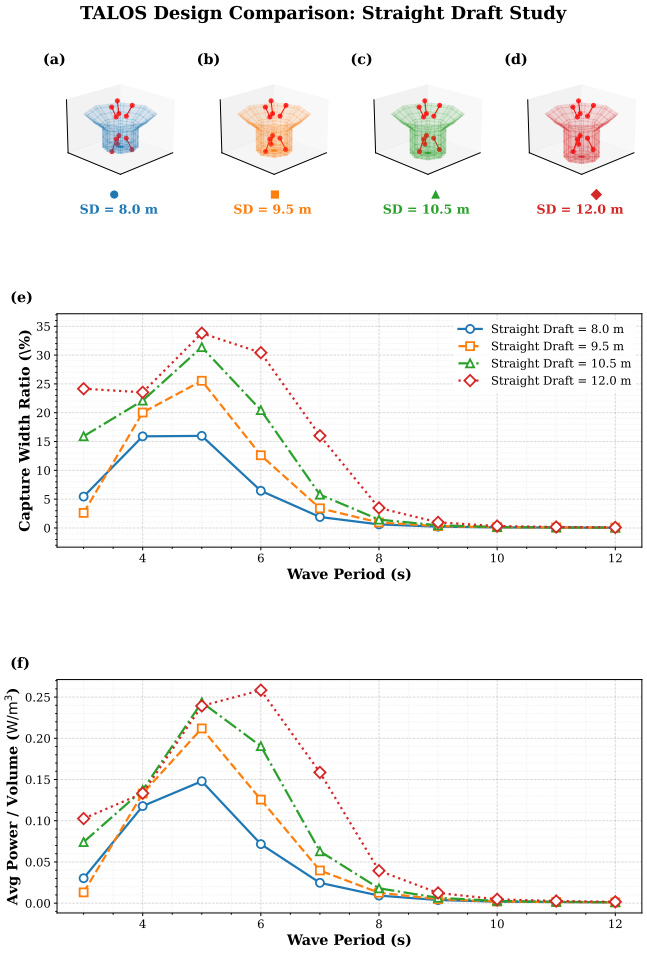

Fig. 5. **Straight Draft Sweep**. **Top:** Top-view mesh profiles (wave direction indicated). **Middle:** Capture width ratio vs. wave period. **Bottom:** Average power per unit volume. Draft values labeled above each geometry.

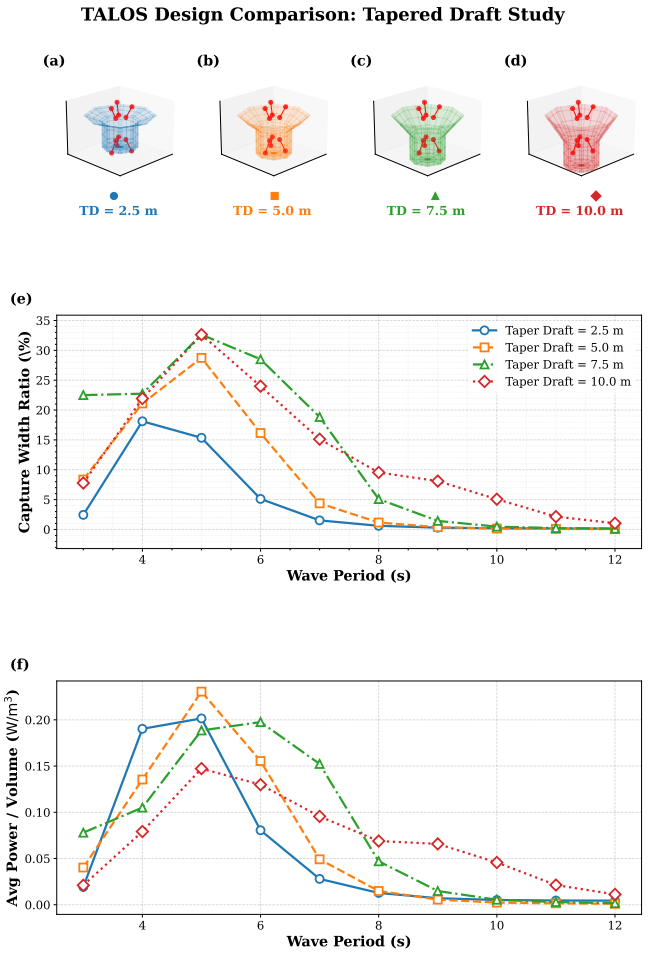

Fig. 6. **Taper Draft Sweep**. **Top:** Mesh profiles for taper height variations. **Middle:** Capture width ratio. **Bottom:** Power per volume. Taper height values labeled above each geometry.

B. Comparison of Geometric Parameter Effects

Figures 5–8 illustrate how variations in hull geometry affect hydrodynamic performance. In each figure, the top row visualizes the geometry, while the middle and bottom plots show performance metrics. Notable trends include:

- **Straight and taper draft:** Increased draft shifts the resonance to longer wave periods and can broaden absorption bandwidth. However, larger volume also increases inertial and damping effects, leading to diminishing returns in power-per-volume. The narrower tapered draft section produces promising results; it is possible that the angle of the tapered section is critical to TALOS' performance.
- **Top radius:** Excessively wide tops reduce both power capture and efficiency, likely due to increased added mass and radiation damping. There is likely some optimal combination of this top radius variable with the tapered draft section.
- **Nose shape:** Forward-protruding noses improve performance at longer periods, while recessed noses favor shorter waves. This reflects the trade-off between excitation efficiency and radiated wave cancellation. The superior performance of flatter nose profiles in our simulations raises an interesting question about potential flow assump-

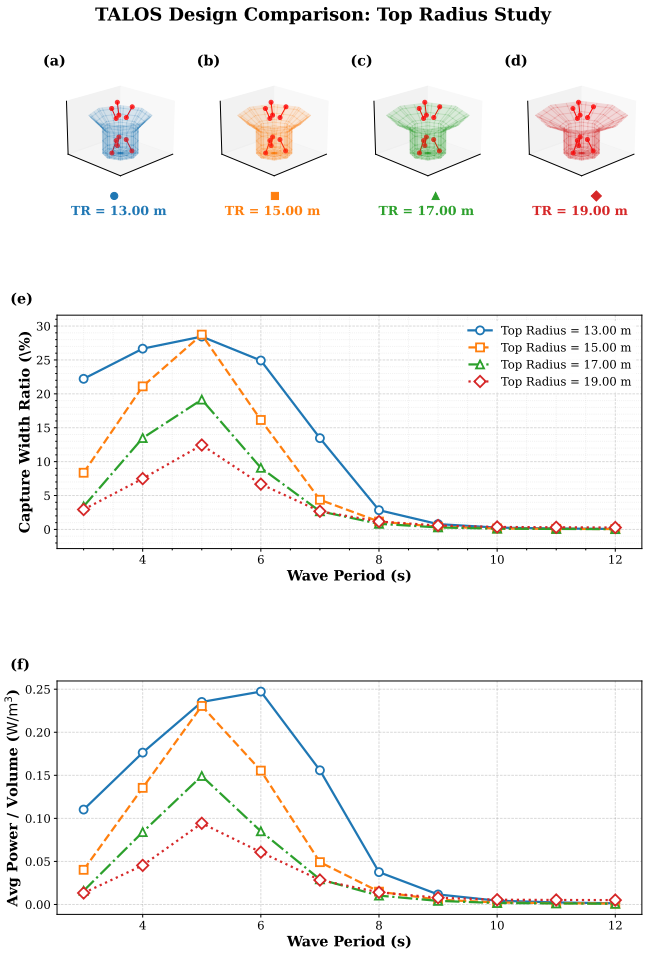

Fig. 7. **Top Radius Sweep**. **Top:** Geometry profiles. **Middle:** CWR trend as radius increases. **Bottom:** Power output normalized by device volume. Radius values labeled above each geometry.

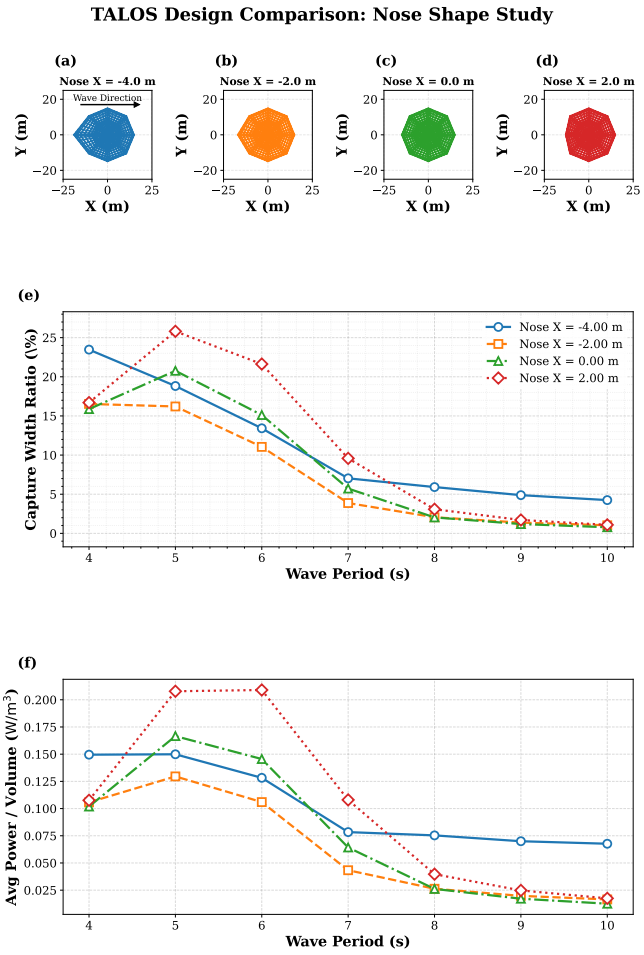

Fig. 8. **Nose Shape Sweep**. **Top:** Nose geometries defined by leading edge x-position. **Middle:** CWR response vs. wave period. **Bottom:** Power-per-volume efficiency. Nose position values labeled above each geometry.

tions: would viscous effects or flow separation alter this behavior? This is precisely the type of insight that could be validated through SEA-Stack's high-fidelity simulations, helping us distinguish between numerical artifacts and genuine physical phenomena.

C. PTO Attachment Sweep: Capture Width Ratio and Power Output

The aggregate power output of the six PTO units is used to analyze the device's overall performance in terms of CWR and normalized power output (power/volume). Figure 9 shows the results for four different PTO attachment configurations. Notably, there is a clear winner—the "Midway In" configuration, which achieves the highest CWR and normalized power output. This suggests that the placement of the PTO attachment points has a significant impact on the device's efficiency.

D. Individual PTO Power Time-Series Analysis

To better understand the origin of the performance differences, Figure 10 presents the time-series power output for each PTO unit in all four configurations. The mesh visualizations at the top clarify the spatial arrangement of the PTOs relative to the wave direction.

A key observation is that the rear PTOs (those oriented in the x-z plane and aligned with the wave direction) consistently produce more power, with the upper rear PTO (PTO 4) dominating the overall performance. The "Midway In" configuration stands out because it enables PTO 4 to achieve its highest output, which largely explains the superior CWR observed in this case.

Additionally, the time series reveal that in the "Midway In" configuration, the power outputs of the PTOs are more in phase, whereas in other configurations the phase matching is less pronounced. This phase alignment could be an important design feature, as it may lead to less smooth aggregate power output when summing across all six PTOs.

These results suggest that future design efforts could focus on further optimizing the placement and tuning of the most productive PTOs (such as PTO 4), or exploring ways to increase the contribution from the other PTO units. Enhancing phase matching across PTOs may also be beneficial for improving the quality and smoothness of the delivered power.

E. Design Insights

These results highlight the value of TOP-WEC as a design tool:

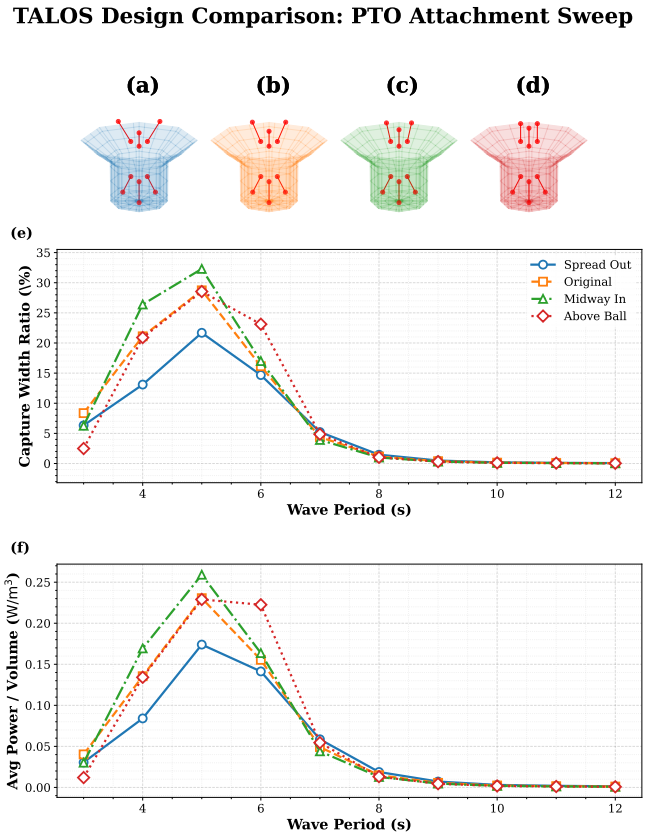

Fig. 9. **PTO Attachment Sweep: Hydrodynamic Performance. Top:** Mesh visualizations of the four PTO attachment configurations. **Middle:** CWR as a function of wave period. **Bottom:** Normalized average power output (power/volume) as a function of wave period. The "Midway In" configuration achieves the highest CWR and power/volume, indicating an optimal PTO placement for this geometry.

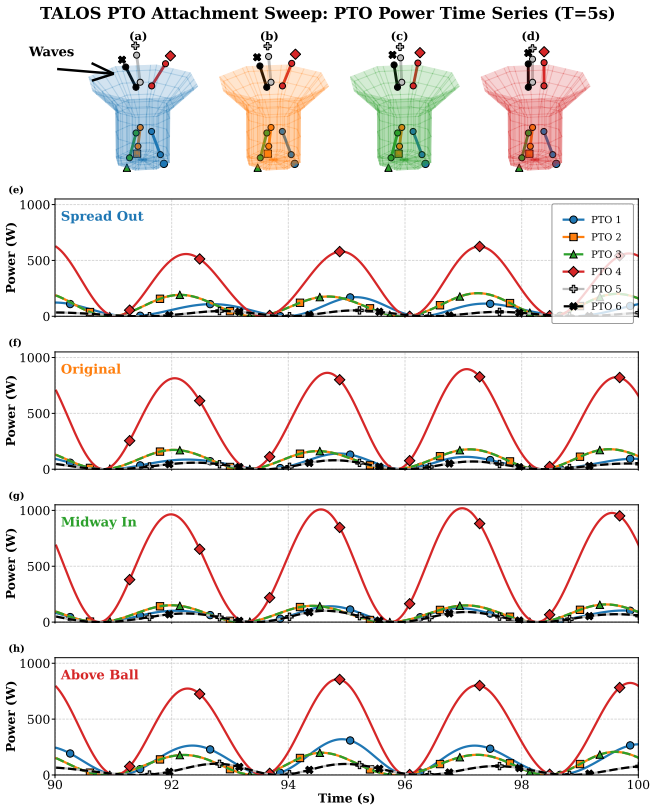

Fig. 10. **Individual PTO Power Time Series. Top:** Mesh visualizations of the four PTO attachment configurations, with wave direction indicated. **Bottom:** Power output time series for each PTO unit in each configuration (T=5 s). The rear PTOs, especially PTO 4, dominate the power output, and the "Midway In" configuration achieves both the highest output and the best phase alignment across PTOs.

- **Volumetric efficiency matters.** Maximizing power-per-volume ensures both performance and compactness—a critical consideration for cost-effective deployment.
- **Geometry matters differently for different wave climates.** Designers can tailor specific features (e.g., nose geometry or taper profile) to align device dynamics with local wave spectra.
- **Multi-parameter tuning is essential.** The observed nonlinear interactions suggest that optimal performance arises from co-design across multiple parameters—not just one at a time.

The findings underscore that optimal performance is likely achieved not by tuning individual parameters independently, but by identifying favorable combinations—such as the interplay between the tapered draft angle and top radius. This insight motivates future multivariable studies to fully exploit the design space and maximize device efficiency.

Ultimately, the finding that certain geometric features (e.g., flatter nose profiles) perform best in potential flow simulations must be interpreted with caution. Only through high-fidelity modeling and experimental validation can we confirm whether these trends persist in practice, ensuring that design decisions are grounded in physical reality rather than numerical artifacts.

IV. Discussion

A. Benefits of the TOP-WEC Stack

The integrated, scriptable nature of TOP-WEC allows for rapid iteration and supports both deterministic studies and formal optimization. By automating the workflow from geometry meshing to time-domain simulation, TOP-WEC significantly reduces the time and effort required for design iterations. This efficiency enables researchers to explore a wider range of design parameters and configurations, leading to more informed decision-making. For instance, in the TALOS WEC case study, the use of TOP-WEC facilitated the evaluation of multiple geometric configurations, resulting in the identification of designs with up to 20% improvement in energy capture efficiency over the baseline TALOS WEC.

B. Interpretability vs. Optimization

A key advantage of structured design exploration is the ability to interpret and understand the relationships between design parameters and performance outcomes. Black-box optimizers may converge on solutions without revealing the underlying trends, whereas a structured design exploration approach enables direct observation of how specific geometric changes—such as nose profile shape—affect power absorption. For instance, we observed that flatter nose profiles consistently yield higher power in our simulations. This

level of interpretability is crucial: it allows us to identify patterns, question unexpected results, and develop physical intuition about the system's behavior.

C. Validation and Confidence Building

However, interpretability alone is not sufficient. The trends we observe—such as the apparent superiority of flatter nose profiles—may be artifacts of the modeling assumptions, particularly the use of linear potential flow theory, which neglects viscous effects and flow separation. If we relied solely on black-box optimization, we might accept such results uncritically, potentially leading to suboptimal or even detrimental design choices. The staged modeling approach enabled by TOP-WEC and, in the future, SEA-Stack, is therefore essential. It will allow us to flag trends of interest during early-stage exploration and then transition promising designs to high-fidelity computational fluid dynamics studies for rigorous validation. This workflow not only improves the quality of design decisions but also builds confidence in simulation results by ensuring that observed performance gains are grounded in physical reality rather than numerical artifacts. As SEA-Stack matures, this integrated pathway will be critical for advancing WEC design and reducing the risks associated with over-reliance on simplified models or automated optimizers.

D. Limitations and Future Work

The primary limitation of this work is its focus on single-variable design exploration studies. While these studies provide valuable initial insights into parameter sensitivities, they cannot capture the complex interactions between parameters that are crucial for optimal WEC design. The project is now moving forward with multivariable design studies in more concentrated regions of the design space, guided by the insights gained from these initial explorations. A key challenge in these more complex studies is presenting the results in an intelligible way that helps designers understand how changes affect system performance. This requires additional work on analyzing how each design modification impacts power absorption across different degrees of freedom (surge, heave, pitch).

On the implementation side, the workflow could be streamlined by having Capytaine write .h5 files directly, eliminating the current conversion step. However, this is complicated by the lack of a clear standard for defining .h5 files for hydrodynamics, which is becoming increasingly important as these files are used across different software platforms (including WEC-Sim, HydroChrono, Capytaine, BEMRosetta). The establishment of a standardized, version-controlled .h5 file structure would be valuable for the community, and is something we are working toward under the SEA-Stack project.

V. Conclusion

We have introduced TOP-WEC, a fully integrated, scriptable software stack for WEC design exploration. By automating the workflow from geometry meshing to time-domain simulation, TOP-WEC enables rapid iteration and supports both deterministic studies and formal optimization. The framework's modular structure and Python-native implementation make it adaptable to various WEC designs and extensible for future enhancements.

Through the TALOS WEC case study, we demonstrated TOP-WEC's capabilities in evaluating multiple geometric configurations and PTO parameters. The results showed significant improvements in energy capture efficiency, highlighting the potential of automated design exploration in advancing WEC technologies toward viable commercial deployment.

Looking forward, TOP-WEC's integration into the broader SEA-Stack ecosystem will enable a comprehensive validation pathway. As SEA-Stack matures, it will provide the high-fidelity simulation capabilities needed to validate promising designs identified through TOP-WEC's rapid exploration. This multi-tiered approach—combining fast iteration with rigorous validation—represents a significant step toward more efficient and reliable WEC development. The establishment of standardized file formats and validation protocols under SEA-Stack will further enhance the framework's utility for the broader WEC community.

References

[1] R. Kempener and F. Neumann, "Ocean energy: *Wave Energy* technology brief," International Renewable Energy Agency (IRENA), Abu Dhabi, United Arab Emirates, Tech. Rep., Jun. 2014, accessed 2025-04-22. [Online]. Available: https://www.irena.org/-/media/Files/IRENA/Agency/Publication/2014/Wave-Energy_V4_web.pdf

[2] Smart Energy International Editorial Team. (2014, Sep.) Wave and tidal power in the energy mix: What is the potential? Accessed 2025-04-09. [Online]. Available: https://www.smart-energy.com/regional-news/north-america/wave-and-tidal-power-in-the-energy-mix-what-is-the-potential/

[3] J. Weber and D. Laird, "Structured innovation of high-performance wave energy converter technology," in *Proceedings of the 11th European Wave and Tidal Energy Conference (EWTEC 2015)*. Nantes, France: NREL & Sandia National Laboratories, Sep. 2015, pp. 1–10, nREL/CP-5000-64744 (printed Jan 2018). [Online]. Available: https://www.nrel.gov/docs/fy18osti/64744.pdf

[4] U.S. Department of Energy, Water Power Technologies Office. (2023) Case study – wave energy prize. Accessed 2025-04-09. [Online]. Available: https://www.challenge.gov/toolkit/case-studies/wave-energy-prize/

[5] B. Guo and J. V. Ringwood, "Geometric optimisation of wave-energy-conversion devices: A survey," *Renewable and Sustainable Energy Reviews*, vol. 145, p. 111324, 2021. [Online]. Available: https://www.sciencedirect.com/science/article/pii/S1364032121004673

[6] J. Davidson and R. Costello, "Efficient nonlinear hydrodynamic models for wave energy converter design—a scoping study," *Journal of Marine Science and Engineering*, vol. 8, no. 1, p. 35, 2020. [Online]. Available: https://www.mdpi.com/2077-1312/8/1/35

[7] R. G. Coe, Y.-H. Yu, and J. van Rij, "A survey of WEC reliability, survival and design practices," *Energies*, vol. 11, no. 1, p. 4, 2018. [Online]. Available: https://www.mdpi.com/1996-1073/11/1/4

[8] L. Papillon, R. Costello, and J. V. Ringwood, "Boundary element and integral methods in potential flow theory: A review with a focus on wave-energy applications," *Journal of Ocean Engineering and Marine Energy*, vol. 6, pp. 303–337, 2020. [Online]. Available: https://link.springer.com/article/10.1007/s40722-020-00175-7

[9] A. Trueworthy and B. DuPont, "The wave-energy converter design process: Methods applied in industry and shortcomings of current practice," *Journal of Marine Science and Engineering*, vol. 8, no. 11, p. 932, 2020. [Online]. Available: https://www.mdpi.com/2077-1312/8/11/932

[10] A. P. McCabe, G. A. Aggidis, and M. B. Widden, "Optimizing the shape of a surge-and-pitch wave energy collector using a genetic algorithm," *Renewable Energy*, vol. 35, no. 12, pp. 2767–2775, 2010. [Online]. Available: https://doi.org/10.1016/j.renene.2010.04.029

[11] A. P. McCabe, "Constrained optimisation of the shape of a wave energy collector by genetic algorithm," *Renewable Energy*, vol. 51, pp. 274–284, 2013. [Online]. Available: https://doi.org/10.1016/j.renene.2012.09.054

[12] D. J. Pizer, "Numerical modelling of wave energy absorbers," University of Edinburgh, Edinburgh, UK, Technical Report EWPP, 1994. [Online]. Available: https://era.ed.ac.uk/bitstream/handle/1842/23532/1994\%20EWPP\%20Numerical\%20models\%20of\%20wave\%20energy\%20absorbers.pdf

[13] S. H. Salter, "Wave energy: Nostalgic ramblings, future hopes and heretical suggestions," *Journal of Ocean Engineering and Marine Energy*, vol. 2, pp. 115–128, 2016. [Online]. Available: https://doi.org/10.1007/s40722-016-0057-3

[14] M. Penalba, G. Giorgi, and F. Dias, "Mathematical modelling of wave energy converters: A review of nonlinear approaches," *Renewable and Sustainable Energy Reviews*, vol. 78, pp. 1188–1207, 2017.

[15] Y.-H. Yu, Y. Li, and K. Ruehl, "Wec-sim phase 1 validation testing — numerical modelling of experiments," National Renewable Energy Laboratory, Tech. Rep. NREL/TP-5000-65836, 2016. [Online]. Available: https://www.nrel.gov/docs/fy16osti/65836.pdf

[16] J. van Rij, Y. H. Yu, and R. G. Coe, "Design load analysis for wave energy converters," National Renewable Energy Laboratory, Golden, CO, USA, Tech. Rep. NREL/CP-5000-71213, 2018. [Online]. Available: https://www.nrel.gov/docs/fy19osti/71213.pdf

[17] J. van Rij, Y. H. Yu, Y. Guo, and R. G. Coe, "A wave energy converter design load case study," *Journal of Marine Science and Engineering*, vol. 7, no. 8, p. 250, 2019. [Online]. Available: https://www.mdpi.com/2077-1312/7/8/250

[18] D. Ogden, K. Ruehl, Y.-H. Yu, A. Keester, D. Forbush, J. Leon-Quiroga, and N. Tom, "Review of wec-sim development and applications," *International Marine Energy Journal*, vol. 5, no. 3, pp. 293–303, 2022, also available at https://www.nrel.gov/docs/fy23osti/83366.pdf. [Online]. Available: https://marineenergyjournal.org/imej/article/view/12

[19] C. Guo, W. Sheng, D. G. D. Silva, and G. Aggidis, "A review of the levelized cost of wave energy based on a techno-economic model," *Energies*, vol. 16, no. 5, p. 2144, 2023. [Online]. Available: https://www.mdpi.com/1996-1073/16/5/2144

[20] C. A. Michelén Ströfer, D. T. Gaebele, R. G. Coe, and G. Bacelli, "Control co-design of power take-off systems for wave energy converters using wecopttool," *IEEE Transactions on Sustainable Energy*, vol. 14, no. 4, pp. 1–11, 2023. [Online]. Available: https://ieeexplore.ieee.org/document/10110979

[21] D. Ogden, N. Tom, J. van Rij, Y. Guo, and Y.-H. Yu, "Numerical modelling of a two-body point absorber featuring variable geometry." National Renewable Energy Lab. (NREL), Golden, CO (United States), 09 2021. [Online]. Available: https://www.osti.gov/biblio/1837966

[22] N. Tom, "Review of wave energy converter power take-off systems, testing practices and evaluation metrics," National Renewable Energy Laboratory, Golden, CO, USA, Conference Paper (Preprint) NREL/CP-5700-82807, 2022, presented at ASME IMECE 2022; Accessed 2025-04-22. [Online]. Available: https://www.nrel.gov/docs/fy23osti/82807.pdf

[23] N. Tom *et al.*, "Non-linear model predictive control for wecs using wec-sim," National Renewable Energy Laboratory, Tech. Rep. NREL/TP-5000-81943, 2022. [Online]. Available: https://www.nrel.gov/docs/fy22osti/81943.pdf

[24] S. Husain, J. Davis, N. Tom, K. Thiagarajan, C. Burge, and N. Nguyen, "Influence on structural loading of a wave energy converter by controlling variable-geometry components and the power take-off," *Journal of Offshore Mechanics and Arctic Engineering*, vol. 145, no. 3, p. 030905, 2023. [Online]. Available: https://asmedigitalcollection.asme.org/offshoremechanics/article/145/3/030905/1160113

[25] Lancaster University. (2025) Talos wave-energy converter. Accessed 2025-04-22. [Online]. Available: https://www.lancaster.ac.uk/engineering/research/talos/

[26] M. Ancellin and F. Dias, "Capytaine: A python-based linear potential-flow boundary element solver," *Journal of Open Source Software*, vol. 4, no. 36, p. 1341, 2019. [Online]. Available: https://doi.org/10.21105/joss.01341

[27] D. Ogden, Z. Quinton, T. de Lataillade, and M. Pallud, "Hydrochrono: An open-source hydrodynamics package for project chrono," National Renewable Energy Laboratory, Tech. Rep. NREL/CP-5700-86719, 2023, conference paper preprint; presented at EWTEC 2023. [Online]. Available: https://www.osti.gov/biblio/2005593